

23 NOV 1977

4000

**NRL Report 8166**

# **Fatigue Crack Propagation Resistance of Beta-Annealed Ti-6Al-4V Alloys of Differing Interstitial Oxygen Contents**

G. R. YODER, L. A. COOLEY, and T. W. CROOKER

*Metals Performance Branch  
Engineering Materials Division*

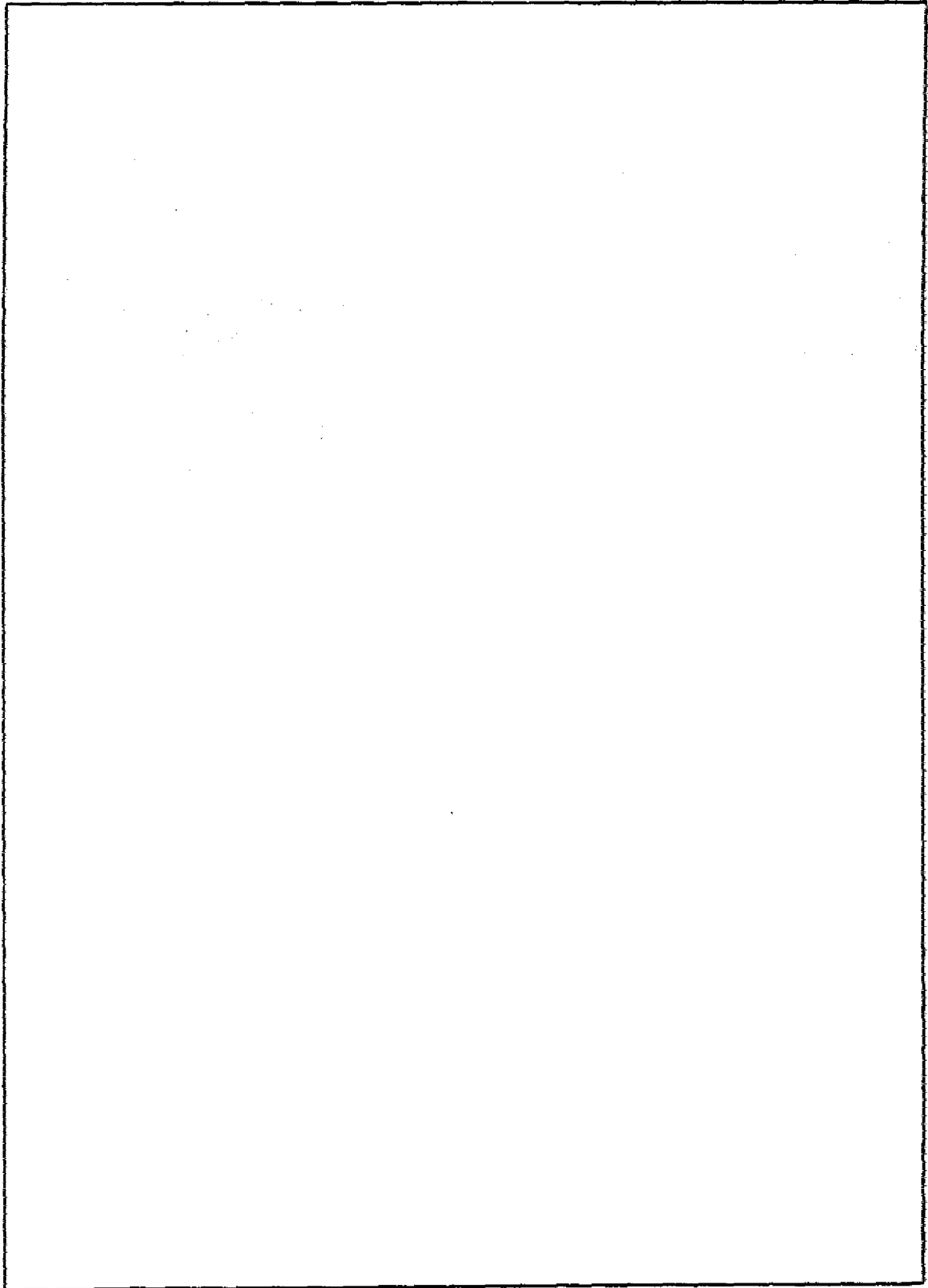
October 4, 1977



**NAVAL RESEARCH LABORATORY**  
Washington, D.C.

Approved for public release; distribution unlimited

REPORT DOCUMENTATION PAGE		READ INSTRUCTIONS BEFORE COMPLETING FORM								
1. REPORT NUMBER NRL Report 8166	2. GOVT ACCESSION NO.	3. RECIPIENT'S CATALOG NUMBER								
4. TITLE (and Subtitle) FATIGUE CRACK PROPAGATION RESISTANCE OF BETA- ANNEALED Ti-6Al-4V ALLOYS OF DIFFERING INTERSTITIAL OXYGEN CONTENTS		5. TYPE OF REPORT & PERIOD COVERED Final report on one phase of a continuing NRL Problem								
		6. PERFORMING ORG. REPORT NUMBER								
7. AUTHOR(s) G. R. Yoder, L. A. Cooley, and T. W. Crooker		8. CONTRACT OR GRANT NUMBER(s)								
9. PERFORMING ORGANIZATION NAME AND ADDRESS Naval Research Laboratory Washington, DC 20375		10. PROGRAM ELEMENT, PROJECT, TASK AREA & WORK UNIT NUMBERS NRL Problem 63M01-24 Project RR 022-01-46								
11. CONTROLLING OFFICE NAME AND ADDRESS Office of Naval Research Arlington, VA 22217		12. REPORT DATE October 4, 1977								
		13. NUMBER OF PAGES 17								
14. MONITORING AGENCY NAME & ADDRESS (if different from Controlling Office)		15. SECURITY CLASS. (of this report) UNCLASSIFIED								
		15a. DECLASSIFICATION/DOWNGRADING SCHEDULE								
16. DISTRIBUTION STATEMENT (of this Report)  Approved for public release; distribution unlimited										
17. DISTRIBUTION STATEMENT (of the abstract entered in Block 20, if different from Report)										
18. SUPPLEMENTARY NOTES										
19. KEY WORDS (Continue on reverse side if necessary and identify by block number)										
<table> <tbody> <tr> <td>Fatigue crack propagation</td> <td>Oxygen content</td> </tr> <tr> <td>Titanium alloys</td> <td>Beta grain size</td> </tr> <tr> <td>Widmanstätten microstructure</td> <td>Reversed plastic zone size</td> </tr> <tr> <td>Beta anneal</td> <td></td> </tr> </tbody> </table>			Fatigue crack propagation	Oxygen content	Titanium alloys	Beta grain size	Widmanstätten microstructure	Reversed plastic zone size	Beta anneal	
Fatigue crack propagation	Oxygen content									
Titanium alloys	Beta grain size									
Widmanstätten microstructure	Reversed plastic zone size									
Beta anneal										
20. ABSTRACT (Continue on reverse side if necessary and identify by block number)										
<p>Fatigue crack growth rates have been determined for beta-annealed Ti-6Al-4V alloys with respective oxygen contents of 0.06, 0.11, 0.18, and 0.20 weight percent. For each of these alloys, transitional crack growth behavior has been observed which appears to correlate with a critical value of the reversed plastic zone size: the Widmanstätten packet size. Moreover, growth rates below transitional levels order in terms of packet size. The present results suggest that interstitial oxygen content and prior beta grain size significantly affect fatigue crack growth rates through control of the Widmanstätten packet size.</p>										



## CONTENTS

INTRODUCTION .....	1
MATERIALS AND PROCEDURES .....	1
RESULTS AND ANALYSIS .....	2
Fatigue Crack Propagation: Transitional Behavior .....	2
Correlation Between Reversed Plastic Zone and Microstructural Dimensions .....	5
Structure-Sensitive, Crystallographic Bifurcation ( $\Delta K \leq \Delta K_T$ ) .....	5
Comparison of Alloy Crack Propagation Rates ( $\Delta K \leq \Delta K_T$ ): A 5-Fold Difference .....	10
Widmanstätten Packet Size: Key to Reduced Growth Rates .....	10
Effects of Oxygen Content and Prior Beta Grain Size .....	10
DISCUSSION .....	12
CONCLUSIONS .....	13
ACKNOWLEDGMENTS .....	13
REFERENCES .....	13



## FATIGUE CRACK PROPAGATION RESISTANCE OF BETA-ANNEALED Ti-6Al-4V ALLOYS OF DIFFERING INTERSTITIAL OXYGEN CONTENTS

### INTRODUCTION

Though it is well known that interstitial oxygen can markedly affect the fracture toughness and uniaxial tensile properties of titanium alloys, the influence of oxygen content on fatigue crack propagation resistance in these alloys is poorly understood. Moreover, the limited data available on this subject appear to be in disagreement [1-3]. Reference 1, for instance, reported a reduction in fatigue crack growth rates with increased oxygen content in commercially pure  $\alpha$ -titanium alloys. On the other hand, subsequent work with  $\alpha$ -titanium alloys, as reported in Ref. 2, indicated the opposite result: an increase in growth rates with increased oxygen content. In harmony with this latter finding, Ref. 3 reported that recrystallization annealed Ti-6Al-4V exhibited increased growth rates with increased oxygen content.

However, no results have been reported to date for the beta-annealed, Widmanstätten microstructure, which has been related to superior fatigue crack propagation resistance in Ti-6Al-4V of commercial purity [3-5]. Accordingly, the purpose of our work is to examine fatigue crack propagation behavior in four beta-annealed Ti-6Al-4V plates with respective oxygen contents of 0.06, 0.11, 0.18, and 0.20 weight percent. For the alloy with 0.20 wt-% oxygen, we reported [5] that fatigue crack growth rates for the  $\alpha/\beta$ -rolled, mill-annealed condition can be reduced by as much as an order of magnitude with a beta anneal, owing primarily to a transition to structure-sensitive crack growth in the Widmanstätten microstructure. We found that the transition corresponds to the point at which the reversed plastic zone attains the average Widmanstätten packet size, with the reduction in growth rates below the transition attributable to crystallographic bifurcation in the Widmanstätten packets.

### MATERIALS AND PROCEDURES

The alloys studied were received in the form of rolled plate, with chemical analyses as given in Table 1. Each alloy was subjected to the following beta anneal [3]: 0.5 hr at 1038°C, cooled to room temperature plus 2 hr at 732°C, cooled to room temperature. This heat treatment was performed in a vacuum furnace, with cooling accomplished in a helium atmosphere at a rate which approximates that in air.

Metallographic samples of each of the resultant Widmanstätten microstructures were polished and etched with Kroll's reagent. From these, some 190 linear intercept measurements of prior beta grain size ( $l_\beta$ ) were made for each alloy, 475 for the Widmanstätten packet size ( $l_{WP}$ ) and 600 for the alpha grain size ( $l_\alpha$ ); a minimum of four photomicrographs was used in each case. Cumulative frequency distributions for  $l_\beta$  and  $l_{WP}$  are exhibited in

Table 1 — Chemical Analyses

Alloy	Content (wt-%)							
	O	Al	V	Fe	N	C	H	Al*
1	0.06	6.0	4.1	0.05	0.008	0.023	0.0050	7.0
2	0.11	6.1	4.0	0.18	0.009	0.02	0.0069	7.6
3	0.18	6.6	4.4	0.20	0.014	0.02	0.0058	8.9
4	0.20	6.7	4.3	0.10	0.011	0.03	0.0060	9.2

Note: Al\* is the aluminum equivalent [6,7]:  $Al^* = Al + \frac{Sn}{3} + \frac{Zr}{6} + 10(O + C + 2N)$ .

Fig. 1, together with mean values ( $\bar{l}_\beta, \bar{l}_{WP}$ ) for each alloy. Figure 2a illustrates the contrast in  $l_\beta$  for alloys 3 and 4, and Fig. 2b illustrates the contrast in  $l_{WP}$  for alloys 1 and 3. Widmanstätten packet sizes range from 17  $\mu\text{m}$  for alloy 1 to 38  $\mu\text{m}$  for alloy 3. Figure 1 shows that one pair of these alloys (alloys 2 and 3) exhibits values of  $\bar{l}_\beta$  which are substantially larger than for the other pair (alloys 1 and 4).

Fatigue crack growth rates ( $da/dN$ ) were determined in ambient air from compact tension specimens of 25.4-mm thickness,  $TL$  crack orientation [8], half-height to width ratio of  $h/W = 0.486$ , and crack length in the range  $0.26 \leq a/W \leq 0.62$ . The stress-intensity ( $K$ ) calibration for the specimen is given in Ref. 9. For each of the four alloys, at least two specimens were subjected to cyclic tension-to-tension loading with a haversine waveform, a frequency of 5 Hz, and a load ratio  $R = P_{\min}/P_{\max} = 0.1$ . The amplitude of loading, though held constant throughout the growth rate test of a given specimen, was different for duplicate specimens, so that data could be generated over different, yet overlapping spectra of stress-intensity range ( $\Delta K$ ). Crack lengths were measured optically on both faces at 15 $\times$  with Gaertner traveling microscopes.

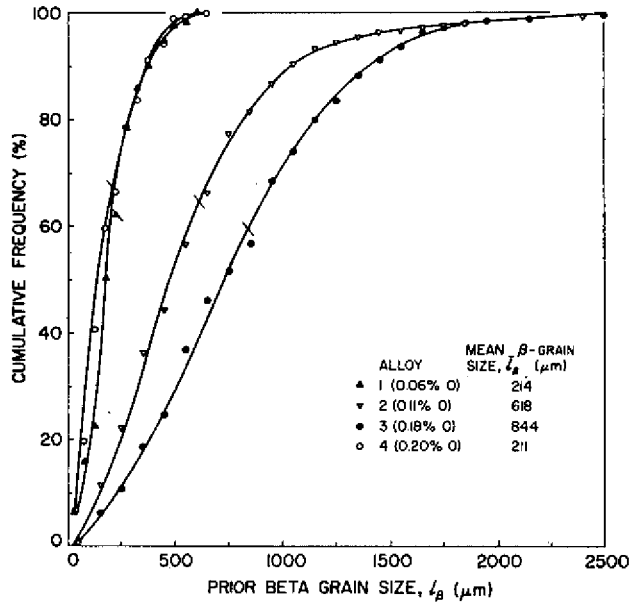
Tests for fracture toughness ( $K_{Ic}$ ) were also made from these compact tension specimens, in accord with ASTM Method E399-74. Tensile properties were determined for the  $T$  and  $L$  orientations from standard 12.8-mm-diameter specimens of 50.8-mm gage length. These mechanical properties are given in Table 2.

## RESULTS AND ANALYSIS

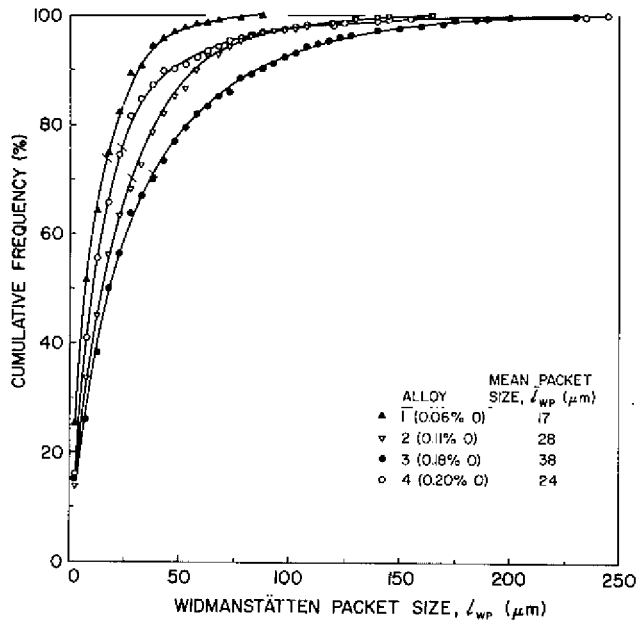
### Fatigue Crack Propagation: Transitional Behavior

Cyclic crack growth rates for alloys 1 through 4 are plotted logarithmically as a function of stress-intensity range in Figs. 3a through 3d respectively. The crack growth behavior of each of the four alloys is distinguished by a clearly defined transition point (indicated by "T" in each figure). At these points the slope or exponent in the growth rate power law [10]

$$da/dN = C(\Delta K)^m \quad (1)$$



(a) Prior beta grain size



(b) Widmanstätten packet size

Fig. 1 — Cumulative frequency distributions (The slash mark on each curve indicates the mean value.)

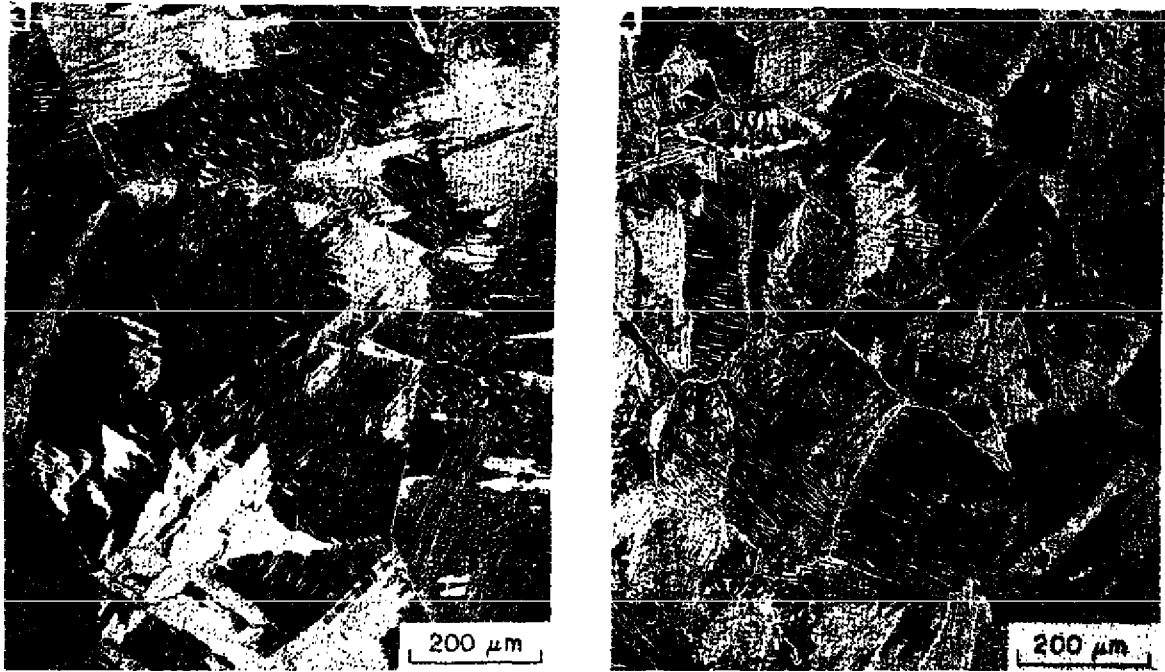


Fig. 2a — Photomicrographs to illustrate contrast in prior beta grain size in alloy 3 (left) and alloy 4 (right)

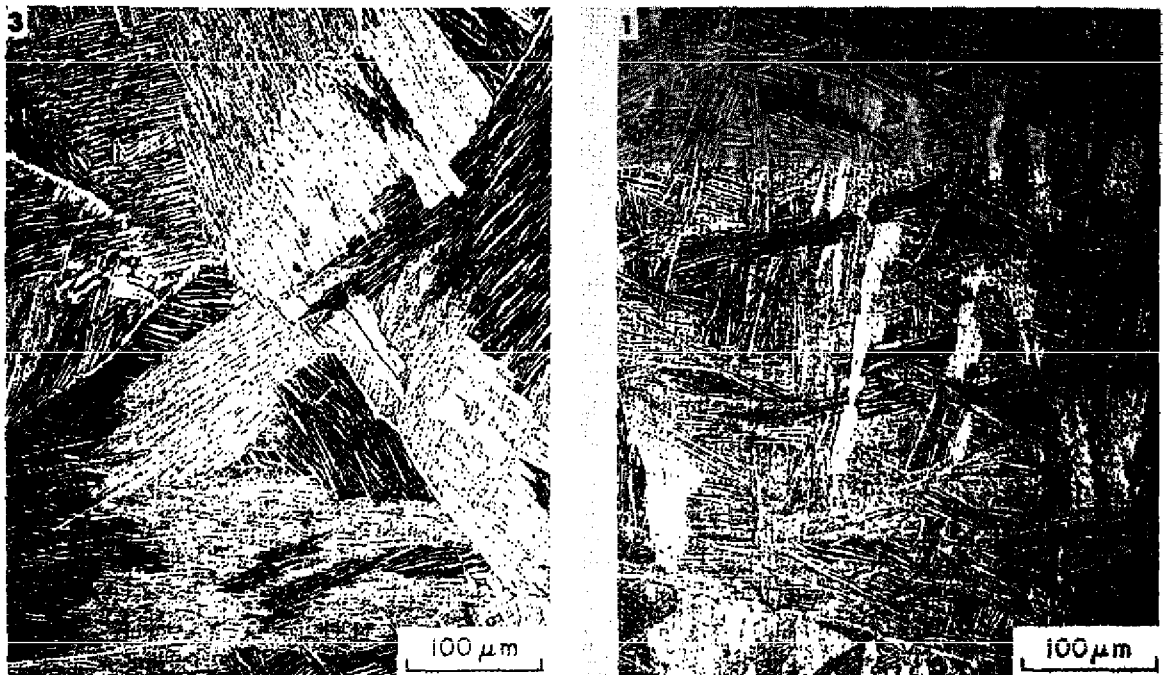


Fig. 2b — Photomicrographs to illustrate contrast in Widmanstätten packet size in alloy 3 (left) and alloy 1 (right)

Table 2 — Mechanical Properties

No.	Alloy		0.2% Yield Strength $\sigma_y$ (MPa)	Tensile Strength $\sigma_{uts}$ (MPa)	Young's Modulus E (GPa)	Reduction in Area (%)	Elongation* (%)	Fracture Toughness $K_{Ic}$ (MPa·m <sup>1/2</sup> )
	Wt-% Oxygen	Orientation						
1	0.06	TL, T	740	818	115	34	10	—
		LT, L	772	829	115	26	10	—
2	0.11	TL, T	772	869	118	19	10	98†
		LT, L	797	867	117	17	8	—
3	0.18	TL, T	818	906	120	13	8	99†
		LT, L	841	931	117	12	8	—
4	0.20	TL, T	869	958	117	16	11	87
		LT, L	892	960	119	23	16	—

\*50.8-mm gage length

†Invalid according to ASTM E399-74

changes by approximately a factor of 2. Transitional values of stress-intensity range ( $\Delta K_T$ ) vary from 18 MPa·m<sup>1/2</sup> for alloy 1 to 27 MPa·m<sup>1/2</sup> for alloy 3, as noted in Table 3.

*Correlation Between Reversed Plastic Zone and Microstructural Dimensions*—The transitional behavior of alloy 4 that we reported elsewhere [5] was attributed to a change from microstructurally sensitive crack growth below the transition to microstructurally insensitive crack growth above the transition; moreover, it was found that the transition corresponded to the point at which the reversed plastic zone size [11-13]

$$r_y^c = 0.132 \left( \frac{\Delta K}{2\sigma_y} \right)^2 \quad (2)$$

attained the average Widmanstätten packet size. The data in Table 3 indicate that this is true also for alloys 1 through 3. In this table, microstructural dimensions are compared to the reversed plastic zone size at the transition point ( $[r_y^c]_T$ ), the latter being calculated through Eq. (2), with  $\sigma_y$  and  $\Delta K_T$  taken from Tables 2 and 3 respectively. For each of the four alloys, the computed value of  $[r_y^c]_T$  agrees well with the respective Widmanstätten packet size; values of  $\bar{l}_\beta$  are approximately an order of magnitude larger than  $[r_y^c]_T$ , and values of  $\bar{l}_\alpha$  are approximately an order of magnitude smaller.

*Structure-Sensitive, Crystallographic Bifurcation ( $\Delta K \leq \Delta K_T$ )*—The similarity in behavior of the four alloys is further illustrated by crack-path sectioning normal to the fracture surface. Below their respective transition points, alloys 1 through 3 exhibit crystallographic bifurcation in the Widmanstätten packets similar to that we noted previously in alloy 4 [5]. Thus within packets that border the Mode I crack plane, multiple parallel cracks appear with a distinct relation to the orientation of  $\alpha$ -phase platelets, as illustrated in Fig. 4. The reduction in growth rates exhibited below the transition points for all four alloys is therefore attributable to this bifurcation, which serves to reduce the effective  $\Delta K$  (and thus  $da/dN$ ) by dispersing the strain field energy of the macroscopic crack among multiple crack tips.

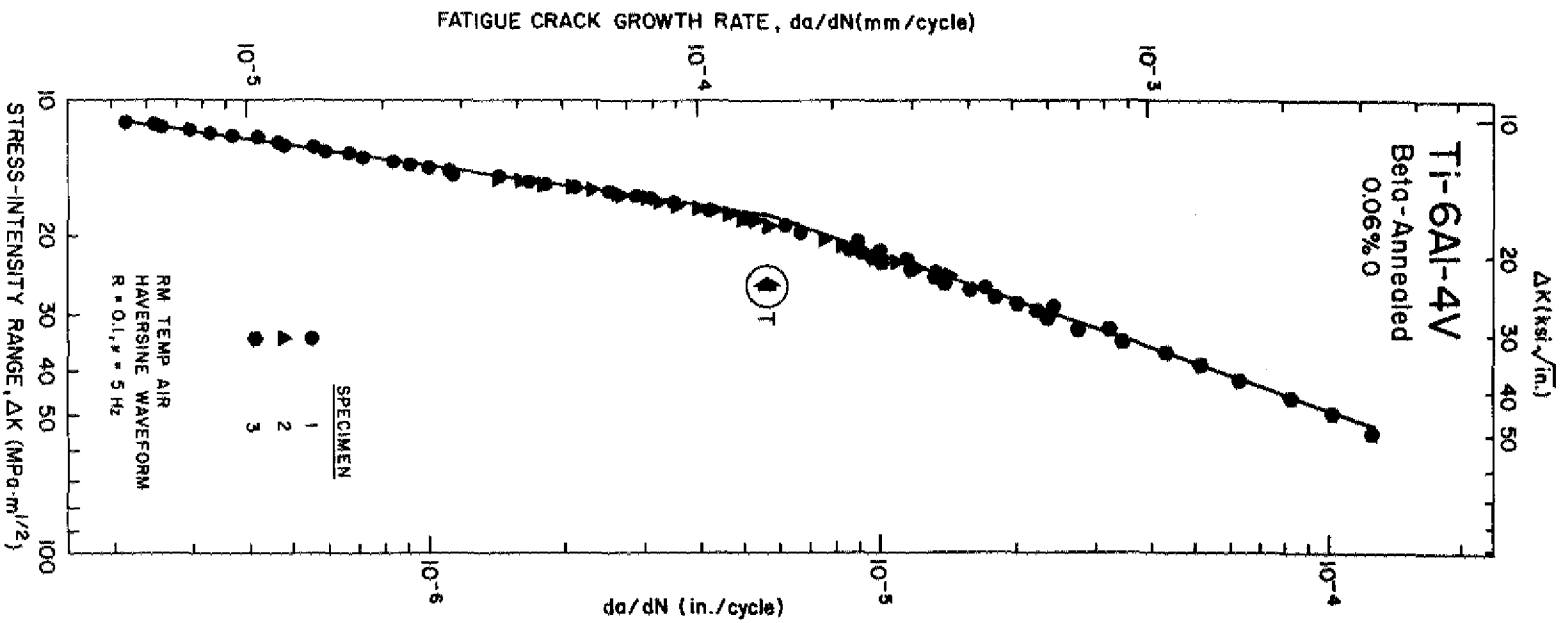


Fig. 3a — Fatigue crack growth rates for alloy 1

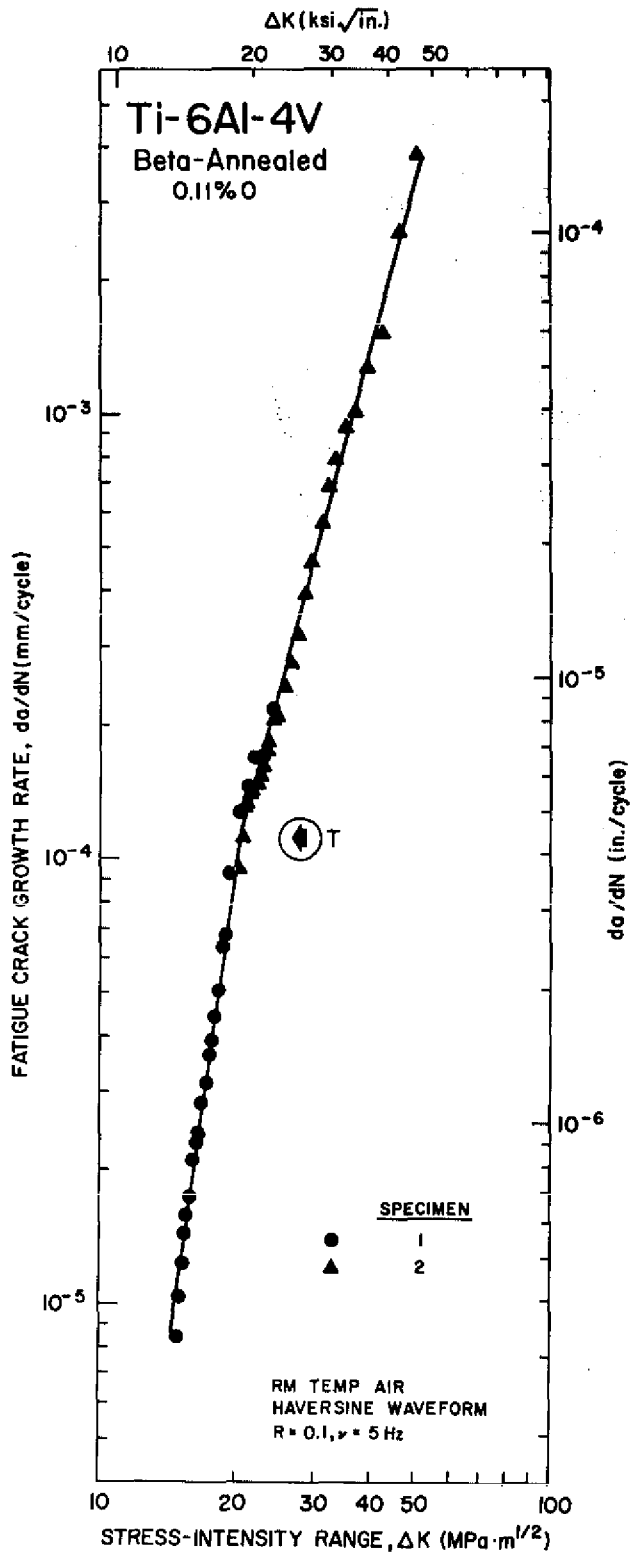


Fig. 3b — Fatigue crack growth rates for alloy 2

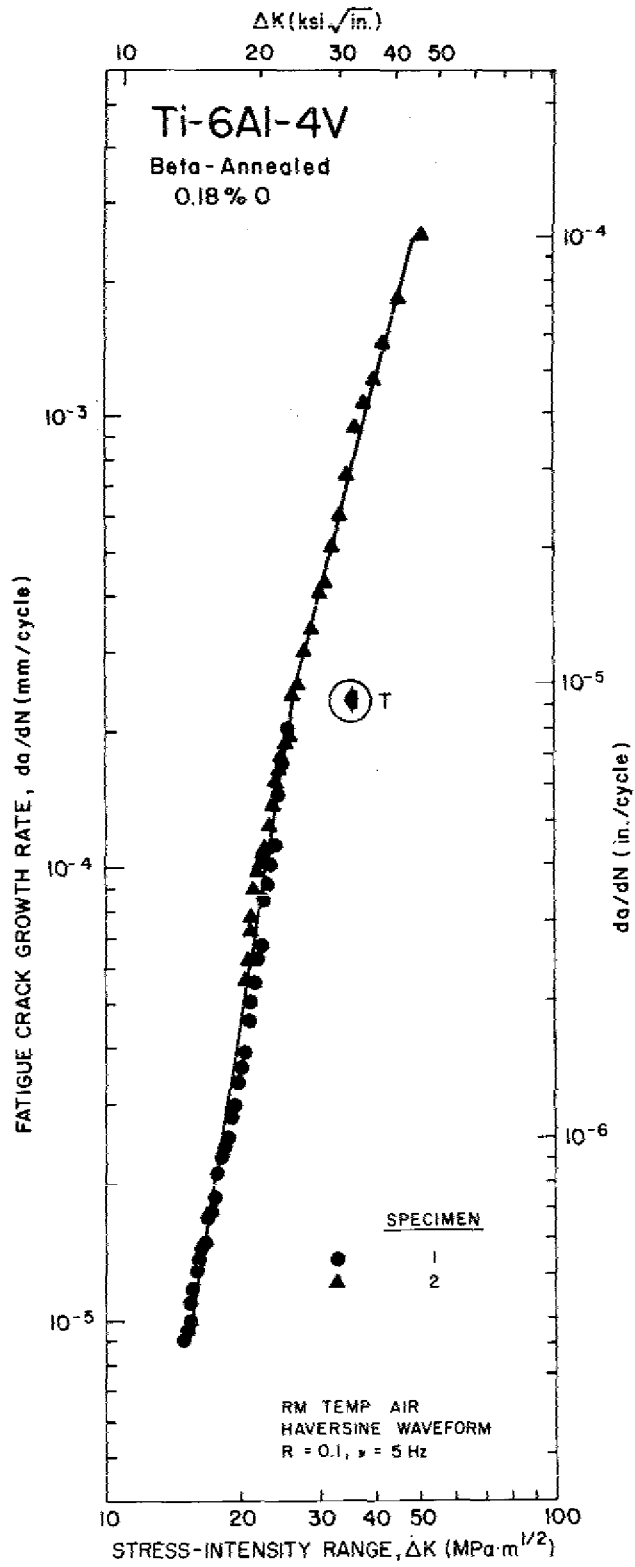


Fig. 3c — Fatigue crack growth rates for alloy 3

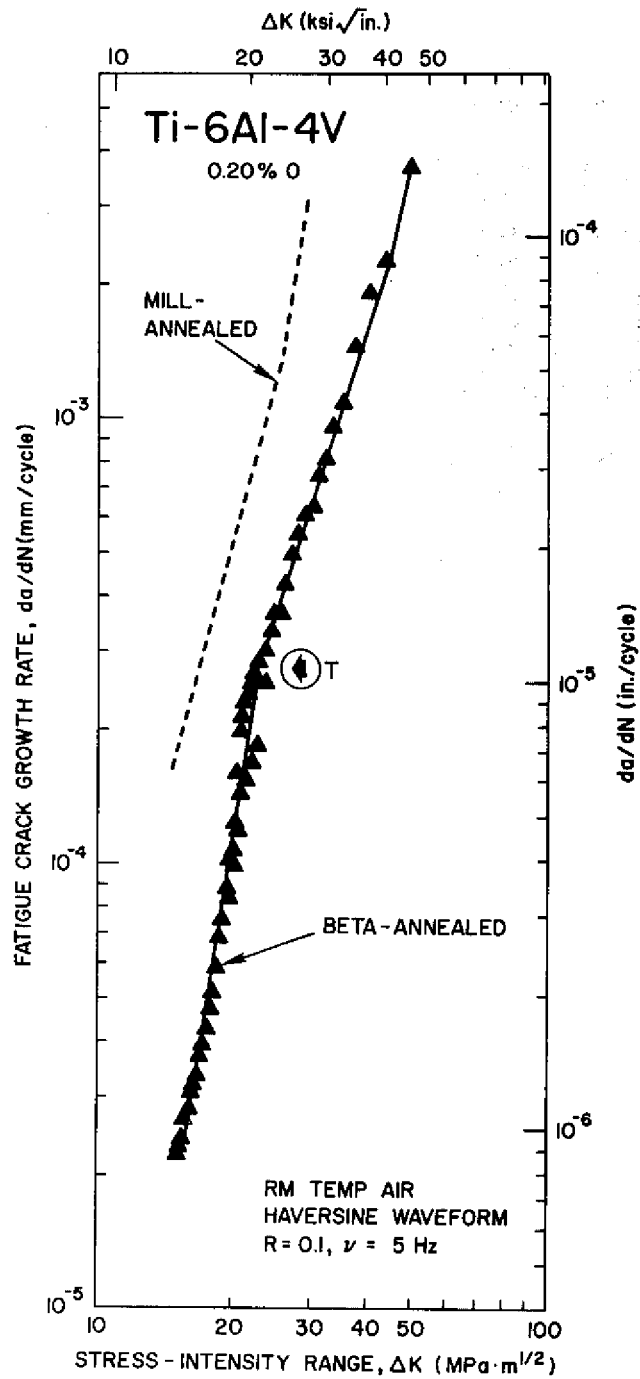


Fig. 3d — Fatigue crack growth rates for alloy 4

Table 3 — Comparison of Transitional Reversed Plastic Zone Size to Microstructural Dimensions

Alloy		Transitional Stress-Intensity Range, $\Delta K_T$ (MPa·m <sup>1/2</sup> )	Transitional Reversed Plastic Zone Size, $[r_y^c]_T$ ( $\mu\text{m}$ )	Microstructural Dimensions ( $\mu\text{m}$ )		
No.	Wt-% Oxygen			$\bar{l}_\alpha$	$\bar{l}_{WP}$	$\bar{l}_\beta$
1	(0.06)	18	19	2	17	214
2	(0.11)	20	23	3	28	618
3	(0.18)	27	35	2	38	844
4	(0.20)	23	23	3	24	211

#### Comparison of Alloy Crack Propagation Rates ( $\Delta K \leq \Delta K_T$ ): A 5-Fold Difference

The trend lines drawn through the data points in Fig. 3 are redrawn in Fig. 5 to facilitate comparison of growth rates for the four alloys.

*Widmanstätten Packet Size: Key to Reduced Growth Rates*—Figure 5 shows that subtransitional crack growth rates order on the basis of Widmanstätten packet size, such that  $da/dN$  decreases with increasing  $\bar{l}_{WP}$ . For example, at  $\Delta K \approx 16 \text{ MPa}\cdot\text{m}^{1/2}$ ,  $da/dN$  is about 5 times less for alloy 3 ( $\bar{l}_{WP} = 38 \mu\text{m}$ ) than for alloy 1 ( $\bar{l}_{WP} = 17 \mu\text{m}$ ). Such behavior may be explained on the premise that, with increasing  $\bar{l}_{WP}$ , the strain-field energy of the macroscopic crack can be spread over increased volumes of material in the crack tip region, thereby further reducing the effective  $\Delta K$  (and thus  $da/dN$ ). This presumes that the bifurcation can extend to the boundaries of Widmanstätten packets that border the Mode I plane (or possibly to some lesser dimension related to the maximum plastic zone size).

*Effects of Oxygen Content and Prior Beta Grain Size*—Further analysis of subtransitional crack growth rates in Fig. 5 leads to the tentative conclusion that interstitial oxygen content, as well as prior beta grain size, significantly affects fatigue crack propagation rates by controlling the subsequent Widmanstätten packet size which develops upon cooling from the beta phase field. Clearly  $da/dN$  does not order on the basis of interstitial oxygen content alone (when all four alloys are considered), but if the alloys are paired on the basis of similar prior beta grain size—alloys 1 and 4 ( $\bar{l}_\beta = 214 \mu\text{m}$  and  $211 \mu\text{m}$  respectively) vs alloys 2 and 3 ( $\bar{l}_\beta = 618 \mu\text{m}$  and  $844 \mu\text{m}$  respectively)—then the pair with the greater  $\bar{l}_\beta$  exhibits the lower growth rates. Yet within each pair the alloy with greater oxygen content exhibits the lower growth rates. Each of these effects is plausible when considered in terms of the transformation kinetics of the  $\beta \rightarrow \alpha$  transformation: An increase in  $\bar{l}_\beta$  could be expected to reduce the  $\alpha$ -phase nucleation rate and thereby serve to increase  $\bar{l}_{WP}$ , if it is assumed that nucleation occurs primarily at the grain boundaries [14]. Moreover, increased oxygen content could be expected to reduce the  $\alpha$ -phase nucleation rate and to enhance the growth rate

the beta anneal has served to equilibrate any preferred orientation of basal planes (which may have existed prior to the anneal) relative to the  $T$  and  $L$  directions [19-21]. Consequently the fatigue crack propagation behavior observed for the  $TL$  crack orientation in alloys 1 through 4 would also be anticipated for the  $LT$  orientation.

## CONCLUSIONS

- In the conventional logarithmic plot of fatigue crack growth rate ( $da/dN$ ) vs stress-intensity range ( $\Delta K$ ), each of the four alloys exhibited a significant change in slope at  $\Delta K_T$ , a transition point at which the reversed plastic zone appears to attain the average Widmanstätten packet size,  $\bar{l}_{WP}$ .
- For  $\Delta K \leq \Delta K_T$ , a crystallographic bifurcation of the Widmanstätten packets occurs, which is responsible for the markedly lower growth rates below  $\Delta K_T$ .
- Comparison of alloys indicates that *the larger the average Widmanstätten packet size, the lower the fatigue crack growth rates*; a 5-fold difference in  $da/dN$  is observed between the most and least resistant of the four alloys.
- The influence of interstitial oxygen (or  $\alpha$ -phase stabilizer content), as well as prior beta grain size ( $\bar{l}_\beta$ ), on fatigue crack propagation resistance appears to be indirect but important, namely to control the size of the average Widmanstätten packet which forms upon cooling from above the beta transus.

## ACKNOWLEDGMENTS

We gratefully acknowledge the experimental assistance of G. W. Jackson, M. L. Ciglely, C. R. Forsht and T. R. Harrison.

## REFERENCES

1. J. L. Robinson and C. J. Beevers, *Met. Sci.* 7, 153-159 (1973).
2. A. W. Thompson, J. D. Frandsen, and J. C. Williams, *Met. Sci.* 9, 46-48 (1975).
3. M. J. Harrigan, M. P. Kaplan, and A. W. Sommer, pp. 225-254 in *Fracture Prevention and Control*, D. W. Hoepfner, editor, Mater./Metalwork. Tech. Ser., No. 3, American Society for Metals, Metals Park, Ohio, 1974.
4. N. E. Paton, J. C. Williams, J. C. Chesnutt, and A. W. Thompson, pp. 4-1 to 4-14, in *AGARD Conference Proceedings 185*, 1976 (available from National Technical Information Service, Springfield, Virginia).
5. G. R. Yoder, L. A. Cooley, and T. W. Crooker, "Observations on Microstructurally Sensitive Fatigue Crack Growth in a Widmanstätten Ti-6Al-4V Alloy," *Met. Trans. A* (in press).
6. H. W. Rosenberg, pp. 851-859 in *The Science, Technology and Application of Titanium*, R.I. Jaffee and N. E. Promisel, editors, Pergamon Press, Oxford 1970.

YODER, COOLEY, AND CROOKER

7. R. I. Jaffee, pp. 1665-1693 in *Titanium Science and Technology*, Vol. 3, R. I. Jaffee and H. M. Burte, editors, Plenum Press, New York, 1973.
8. R. J. Goode, *Mater. Res. Stand.* 12, (No. 9) 31-32 (1972).
9. W. G. Clark, Jr., and S. J. Hudak, Jr., *J. Test. Eval.* 3, 454-476 (1975).
10. P. C. Paris and F. Erdogan, *Trans. ASME, J. Basic Eng., Series D*, 85, 528-533 (1963).
11. P. C. Paris, pp. 107-127 in *Fatigue-An Interdisciplinary Approach*, J. J. Burke, N. L. Reed, and V. Weiss, editors, Syracuse University Press, 1964.
12. J. R. Rice, pp. 247-309 in *Fatigue Crack Propagation*, ASTM STP 415, American Society for Testing and Materials, Philadelphia, 1967.
13. G. T. Hahn, R. G. Hoagland, and A. R. Rosenfield, *Met. Trans.* 3, 1189-1202 (1972).
14. R. I. Jaffee, pp. 65-163 in *Progress in Metal Physics*, Vol. 7, B. Chalmers and R. King, editors, Pergamon Press, New York, 1958.
15. M. K. McQuillan, *Met. Rev.* 8, 41-104 (1963).
16. D. J. DeLazaro and W. Rostoker, *Acta Met.* 1, 674-678 (1953).
17. I. S. Polkin and O. V. Kasparova, pp. 1521-1534 in *Titanium Science and Technology*, Vol. 3, R. I. Jaffee and H. M. Burte, editors, Plenum Press, New York, 1973.
18. J. C. Chesnutt, C. G. Rhodes, and J. C. Williams, pp. 99-138 in *Fractography—Microscopic Cracking Processes*, C. D. Beachem and W. R. Warke, editors, ASTM STP 600, American Society for Testing and Materials, Philadelphia, 1976.
19. A. W. Bowen, *Mater. Sci. Eng.* 29, 19-28 (1977).
20. M. J. Harrigan, A. W. Sommer, P. G. Reimers, and G. A. Alers, pp. 1297-1320 in *Titanium Science and Technology*, Vol. 2, R. I. Jaffee and H. M. Burte, editors, TMS-AIME, Plenum Press, New York, 1973.
21. F. Larson and A. Zarkades, Report MCIC-74-20, Metals and Ceramics Information Center, Battelle-Columbus Laboratories, Columbus, Ohio, June 1974.